Structural Transitions of Electrosprayed Ubiquitin Ions Stored in an Ion Trap over ~10 ms to 30 s†

Sunnie Myung, Ethan R. Badman,‡ Young Jin Lee, and David E. Clemmer*

Department of Chemistry, Indiana University, Bloomington, Indiana 47405

Received: March 6, 2002; In Final Form: June 27, 2002

Structural transitions of the +6 to +8 charge states of ubiquitin produced by electrospray ionization have been studied in the gas phase by a new ion trap/ion mobility-mass spectrometry technique. The approach allows transitions to be examined in detail over ~10 ms to 30 s trapping times. This time regime is intermediate between the ~1 to 5 ms time scales of previous mobility measurements [*J. Am. Soc. Mass Spectrom.* **1997**, *8*, 954] and minute to hour time scale measurements associated with trapping experiments done in a Fourier transform mass spectrometer [*Int. J. Mass Spectrom.* **1999**, *185/186/187*, 565]. The results show that over the entire time range, the +6 charge state is dominated by compact structures (with cross sections that are near the value expected for folded states in solution). The +7 state shows evidence for at least two types of initial compact structures. One state (~65% of the population) rapidly unfolds to partially folded and elongated conformers after ~30 to 40 ms. The remaining 35% of ions also unfolds at a much slower rate. The +8 charge state appears to be formed initially in a range of partially folded states. These states rapidly unfold into elongated structures that persist to the longest trapping times that are employed. These results are compared with the longer time scale measurements, and attempts are made to correlate the features observed in the different experiments.

Introduction

Protein structures and folding are influenced by a range of intramolecular and solvent−molecule interactions.[1] Experiments that delineate how different types of interactions influence folding pathways and structures are difficult because of the complexities associated with such large systems. With the advent of electrospray ionization (ESI)[2] it is possible to extract proteins from solution and examine conformations of isolated protein ions. Studies of unsolvated proteins in the gas phase provide direct information about intramolecular interactions.[3] Addition of water to the anhydrous ions,[4] or studies in which the ESI drying process is not carried out to completion, can provide direct information about partially hydrated states.[5,6] Some exciting questions regarding the influence of the presence of a few water molecules on structure can in principle be examined by adding or removing water molecules in a one-at-a-time fashion.

In the present paper, we examine the conformations of the +6 to +8 charge states of ubiquitin ions. We[7,8] and others[9−14] have investigated this system previously and find evidence for multiple conformations of the anhydrous ions in the gas phase. Here, we follow these conformers as they evolve from states that are formed initially by ESI into new gas-phase structures over a 10 ms to 30 s time scale. This is done by storing the protein ions in an ion trap for variable time periods and then examining the shapes of different conformations and charge states by combined ion mobility and mass spectrometry (MS) techniques—an approach that we described recently and used to study cytochrome *c*.[15] Gas-phase structures for different charge states appear to emerge from several pathways, and a simple mechanism showing how different structures appear to be related is proposed.

An additional motivation of the current work is to link structural information obtained over short time scales in mobility experiments with data obtained using other experimental approaches. The ubiquitin system is a good reference point for these types of studies. Bowers' group[11] and our group[7,8] have now investigated this system over short time scales (~1 to 5 ms) using ion mobility techniques; Marshall,[12] McLafferty,[13] and their co-workers have probed conformations at longer times (minutes to hours) using FTMS methods. Purves et al.[14] have combined gas flows with asymmetric oscillating electric fields as a means of selecting different conformers prior to entering the mass spectrometer (an approach referred to as FAIMS). The present report of measurements in the ~10 ms to 30 s time regime allows an additional comparison between different approaches to be made. The results indicate that ions initiate from solution as relatively compact (folded) structures and then exhibit several types of structural transitions. Some transitions appear to occur abruptly (after trapping times of ~35 to 50 ms), producing either partially folded or elongated structures. Other transitions occur over much longer time periods. The new insight helps to bridge gaps in understanding the shorter and longer time scale experiments.

Experimental Section

Ion mobility techniques have been described in detail previously.[16] Only a brief discussion of these methods is given here. A schematic diagram of the ion trap/ion-mobility/quadrupole mass spectrometer used in these studies is shown in Figure 1. This experimental configuration is almost identical to one we described in detail previously.[15] Briefly, positively

† Part of the special issue "Jack Beauchamp Festschrift".

* Corresponding author.

‡ Present address: Chemistry Dept., Purdue University, West Lafayette, IN 47907.

10.1021/jp0206368 CCC: $22.00
Published on Web 08/16/2002

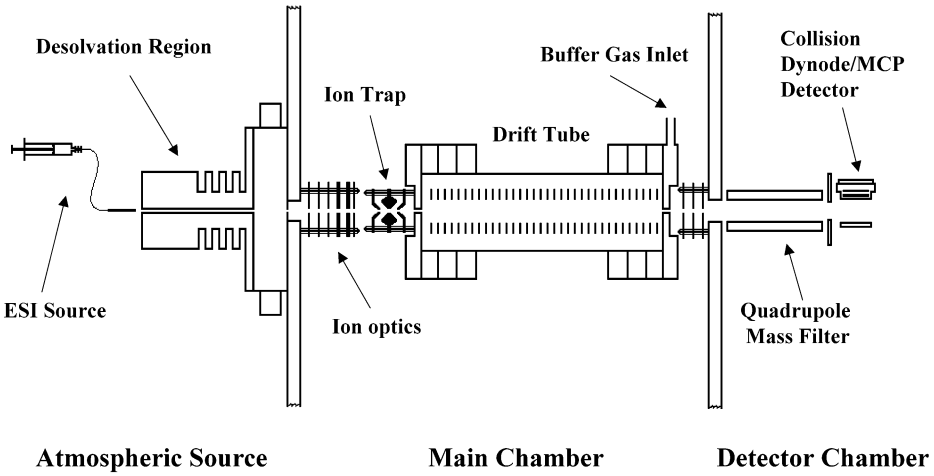

Figure 1. Schematic diagram of the experimental ion trap-ion mobility-mass spectrometry instrument.

charged (protonated) ions are formed by atmospheric pressure electrospray of a solution containing $\sim 10^{-5}$ M of ubiquitin (bovine, Sigma) in 49:49:2 (% volume) water/methanol/acetic acid. Ions are extracted from a differential pumping region and focused in a quadrupole ion trap (RM Jordan, model C-1251). The pressure inside the trap is $\sim 5 \times 10^{-4}$ Torr of 300 K helium. Ions are accumulated in the trap for short times and stored for $\sim$10 ms to 30 s before being ejected from the ion trap into the drift tube. The drift tube is 50.6 cm long with a uniform electric field of 12.8 V cm^{-1} and is operated with $\sim$2.0 Torr of helium buffer gas.

Ion mobility distributions are obtained by recording the time for a pulse of ions to travel through the drift tube and reach the detector. The mobility of the ion is a measure of how fast the ion moves through a gas under the influence of a uniform electric field in a drift tube.[17] An ion with a large average cross-section undergoes more collisions with the buffer gas, and thus has longer drift times than an ion with a smaller average cross section. In favorable cases, comparisons of experimental mobility with calculated values for model structures can provide information about structure. By trapping protein ions for a varying time, information about the kinetics and dynamics of structural transitions can be obtained. Ions that exit the drift tube enter a quadrupole mass filter (Extrel). The quadrupole can be scanned to obtain a mass spectrum or fixed to pass a single charge state. Ions are detected using an off axis collision dynode/microchannel plate system that was constructed in house.

Pulse Sequence for Storing Ions in the Trap and Recording Mobility Distributions. Key to this experiment is the ability to store ions for a variable amount of time.[15] This is accomplished using the pulse sequence shown in Figure 2. In this scheme, a deflector lens is used to gate ions into the trap. The gate time is 5% of the trap delay time. After a variable trap delay ($\sim$10 ms to 30 s for these studies), ions were ejected from the trap into the ion mobility instrument. The total drift time acquisition period is 10 ms.

Experimental Collision Cross Sections. Experimental collision cross sections (Ω) are determined using the relation[14]

$$\Omega = \frac{(18\pi)^{1/2}}{16}\frac{ze}{k_B T}\left[\frac{1}{m_I}+\frac{1}{m_B}\right]^{1/2}\frac{t_D E}{L}\frac{760}{P}\frac{T}{273.2}\frac{1}{N} \quad (1)$$

where z, e, m_I, and m_B correspond to the charge state, electron charge, and masses of the ion and buffer gas, respectively, and N and k_B correspond to the neutral number density and Boltzmann's constant, respectively. The experimental variables

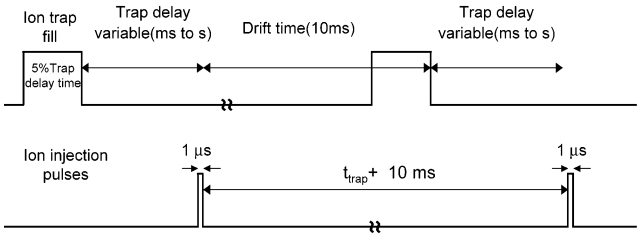

Figure 2. Experimental timing diagram showing the sequence of pulses that is used to accumulate and store ions in the trap and subsequently record ion mobility distributions. Pulses shown in the upper trace are applied to a set of deflector lenses that are situated between the ion source and the trap. The synchronized pulses shown in the lower trace are used to eject ions out of the trap and initiate mobility measurements. See text for details.

E (electric field strength), L (drift tube length), P (buffer gas pressure), and T (buffer gas temperature) are precisely controlled such that any two measurements of the drift time (t_D) usually agrees to within $\sim$1% relative uncertainty.[19]

Results and Discussion

Temperature of Ions Stored in the Ion Trap and Influence of the Energy Used to Inject Ions into the Drift Tube. As discussed previously,[15] an important consideration in these experiments is the temperature of ions stored in the ion trap. Although it is not possible to measure the internal temperature of the ions directly in these studies, we have attempted to minimize internal excitation. The high-pressure ESI source operated at 300 K should produce ions that are near room temperature. Upon exiting the high-pressure source, ions travel $\sim$10 cm at $\sim 5 \times 10^{-5}$ Torr. Collisional excitation is minimized by using a low bias voltage ($\sim$3 to 5 V) to focus ions from the source into the trap. The entrance and exit endcaps and ring electrode of the trap are fixed to the same DC-potential in order to minimize excitation along the axis of the beam. Under these conditions, the ions entering the trap undergo a mild collisional dampening process and should rapidly equilibrate to the temperature of the helium buffer gas (300 K).[20] Several experimental results suggest that the collisional activation of ions upon injection and storage in the trap as well as injection into the drift tube is minimal. Most important to the present work is that compact conformations for the +7 and +8 charge states are observed at short trapping times. Our previous studies[21] and the recent work of Bowers' group[11] show that this would not be the case if ions underwent a substantial collisional activation process before the mobility measurement.

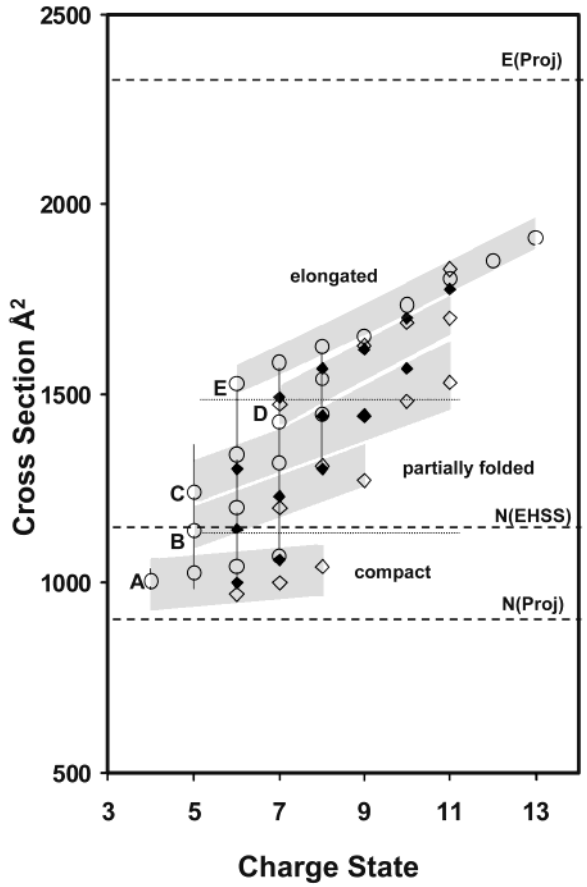

Figure 3. Collision cross sections for the +4 to +13 charge states of ubiquitin ions measured under several different experimental conditions, reported previously in refs 7 and 8. The open circles correspond to data recorded using a range of injection energies an injected ion drift tube (analogous to the instrument used in the present study). The +4 and +5 charge states were formed by proton transfer reactions using an instrumental design that incorporated a gas cell at the exit of the ESI source. The +6 to +13 charge states were formed directly by ESI. The original data (and subsequent studies) have been reanalyzed and it is now possible to resolve additional features in the distributions for +7 and +8 ions, which were not resolvable in the original report (refs 7 and 8). The vertical lines through the open circles show a range of cross sections that are associated with unresolved features in the ion mobility distributions. Also shown are cross sections for the +6 to +11 charge states, recorded at several source temperatures in a high-pressure drift tube, upon electrospraying a 49:49:2 water/aceteonitrile/acetic acid solution (solid diamonds) and a 89:9:2 solution (open diamonds). Overall trends in ion mobility peak shapes and cross sections as a function of charge state suggest that five different conformer types (A though E) are present, indicated by the gray regions in the figure. Finally, dashed lines indicate cross sections that are calculated from coordinates for the crystal structure by two methods (see text) as well as a nearly linear structure.

Summary of Cross Section Results for Ubiquitin Ions. Collision cross sections for ubiquitin ions have been measured under a variety of conditions; a summary of values for the +4 to +13 charge states (recorded using injected-ion and high-pressure drift tube techniques) is shown in Figure 3. Experimental cross sections range from ~1000 Å^2 for the most compact states (observed for the +4 to +7 charge states) to ~1900 Å^2 for the highest charge state (+13). These values for compact states are near calculated values for the compact crystal structure N(Proj) and N(EHSS) in Figure 3. The cross sections for high charge states are consistent with elongated geometries; however, these values are much smaller than values that are calculated for near-linear geometries (E(Proj) in Figure 3).

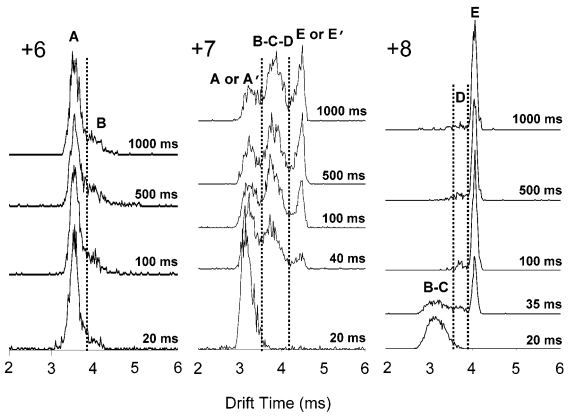

Figure 4. Drift time distribution for the +6 through +8 ions of ubiquitin. The +6 ions were recorded using trapping delay times of 20, 100, 500, and 1000 ms; the +7 ions were recorded using trapping delay time of 20, 40, 100, 500, and 1000 ms; and the +8 ions were recorded using trapping time of 20, 35, 100, 500, and 1000 ms. Dotted lines show the positions of different conformer types. See discussion in text and Figure 3.

In our initial report of this system,[7] we divided the families of cross sections into three conformer types: (1) a compact (folded) state that is observed at low injection energies (<500 eV) for the +6 and +7 charge states, with collision cross sections that are near the Ω(proj) = 930 Å^2 and Ω(EHSS) = 1162 Å^2 values that are calculated from coordinates for the crystal structure; (2) partially folded states, having cross sections between 1120 and 1500 Å^2 that are favored at intermediate injection energies for +6 and +7 ions and low injection energies for the +8 charge state; and, (3) elongated states, with cross sections in excess of 1500 Å^2 that are favored at high-injection energies (>750 eV) for the +6 to +8 charge states. Overall, as has now been discussed many times, the changes in which structures are observed as charge state is increased, compact (+4 to +7) → partially folded (+5 to +9) → elongated (+6 to +13) can be understood by noting that elongated structures can reduce repulsive columbic interactions.

Subsequent studies and the time-dependent measurements presented below indicate that the ubiquitin system is somewhat more complex than the three-state model proposed initially. Under some of the experimental conditions that have been employed, it is possible to resolve additional features in the ion mobility distributions that previously were associated with a broad peak characteristic of partially folded structures. We now divide the cross sections into five different conformer families. Additionally, the time-dependent data presented below allow some states that have identical cross sections to be resolved. To indicate this, we label the families of cross sections in Figure 3 as A (compact or folded), B, C, and D (partially folded), and E (elongated), and use primes (e.g., A′ and A″) to denote those states with indistinguishable cross sections that can be delineated because of their time-dependent behavior.

Ion Mobility Distributions for the +6 to +8 Charge States at Different Trapping Times. Figure 4 shows representative ion mobility distributions obtained upon storing ions in the trap for either 20, 100, 500, or 1000 ms for the +6 charge state; 20, 40, 100, 500, or 1000 ms for the +7 charge state; and 20, 35, 100, 500, or 1000 ms for the +8 charge state. Experimental cross sections, obtained by combining the measured drift times with the experimental parameters (using eq 1) are in good agreement with the values determined in our previous injected ion studies, allowing features to be assigned to the different conformer types described above.

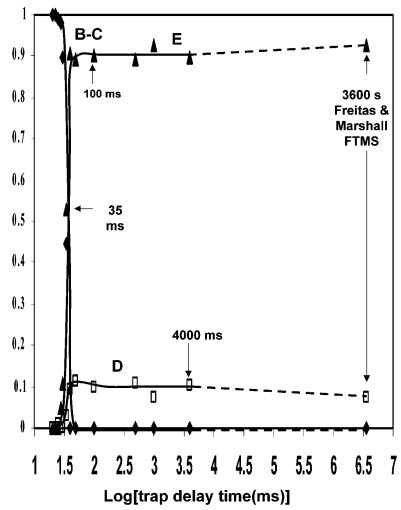

Figure 5. Relative populations of different conformer types for the +8 charge state as a function of the trapping delay time. States B and C are shown as solid diamonds. Populations of states D and E are shown as open squares and solid triangles, respectively. Populations of different conformers from FTMS isotopic exchange studies are shown for a single time point (3600 s). See ref 12 and discussion in text for details.

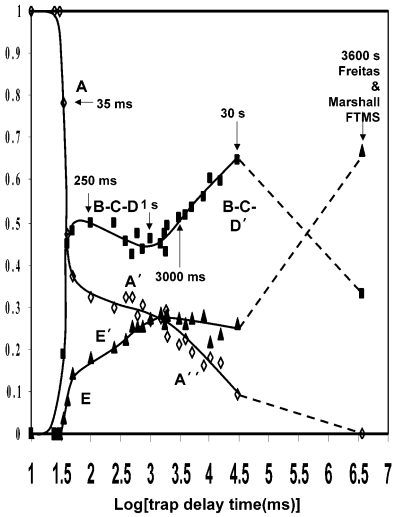

Figure 6. Relative populations of different conformer types for the +7 charge state as a function of the trapping delay time. The compact state A is shown as open diamonds. Populations of partially folded B, C, and D states are shown as solid squares, and the elongated state E is shown as solid triangles. Populations of different conformers from FTMS isotopic exchange studies are shown for a single time point (3600 s). See ref 12 and discussion in text for details.

The three charge states that are shown exhibit fairly different behavior. At all trapping times, distributions for the +6 ion are dominated by a large peak at 3.54 ms, corresponding to the compact A state; the smaller, reproducible tail that extends from ~3.9 ms to ~4.3 ms corresponds to partially folded B ions. At different trapping times there is a small reproducible change in the relative abundances of the A and B states. At short trapping times, <20 ms, the B ions comprise only ~15% of the distribution; there is a small, reproducible increase in this fraction as the trapping time is increased, up to a maximum of ~20% at trapping times of 1 s. We estimate a unimolecular depletion rate constant for the compact state of ~0.2 s^{-1}.

The +7 and +8 charge states show more dramatic changes in populations at shorter times. Below ~30 ms, the distribution for the +7 ions is dominated by a single broad peak at 3.12 ms that is assigned to the compact A state. This peak is too broad to correspond to a single conformer. Thus, multiple compact A conformers must be stable over ms time scales of the drift time measurement. At longer trapping times, ~30 to 50 ms, the fraction of compact A ions abruptly decreases from 100% of the population to ~30 to 40%. During this time, two new peaks with maxima at 3.76 and 4.50 ms, respectively, are observed; an example is shown for a trapping time of 100 ms. The feature at 3.76 ms is broad, and can be assigned to partially folded B, C, and D ions. The sharper peak at 4.50 ms is assigned to elongated E ions. As the trapping time is extended beyond 100 ms, the fraction of compact A continues to decrease (albeit at a substantially slower rate); at ~1 s, ~20 to 30% of the ion distribution remains compact. The observation that some compact A ions rapidly unfold, while others remain stable for extended times requires that at least two types of compact states are present: state A that is depleted at a rate of ~50 s^{-1} and a compact form, A′, that persists to longer times.

Ion mobility distributions for the +8 charge state show a broad feature centered at ~3.2 ms (partially folded B and C state ions) at short trapping times (e.g., 20 ms). As the trapping time is extended, the distribution is dominated by a single sharp peak at 4.05 ms (elongated E state ions). These data also show a small population of ions at 3.82 ms (partially folded D ions).

Relative Populations as a Function of Trapping Time and Comparisons with Other Experimental Approaches. Figures 5 and 6 show the populations of different conformers as a function of trapping time for the +7 and +8 charge states, respectively. We do not show a plot of data for the +6 charge state because only minor changes in the populations are observed (Figure 4). However, the relatively long lifetime that must be associated with the compact +6 charge state is consistent with the very wide dispersion in isotopic exchange recorded by FTMS, even after 1.0 h exchange times.[12] Overall, it appears that structural transitions in the +6 ions are extremely slow, and it is possible that the compact conformer observed in these studies persists even at the extended time scales associated with the FTMS measurement.

The populations in Figures 5 and 6 (for the +8 and +7 charge states, respectively) are plotted on a logarithmic time axis, allowing us to consider a wide range of trapping times ~10^1 to ~10^7 ms. Although the longest trapping time used in these studies is only 30 s, it is worthwhile to extend the plot to substantially longer times so that comparisons to FTMS results can be made. Populations were obtained by integrating regions in the ion mobility distributions that correspond to the different states (Figure 4). A typical plot of the time profile of different conformations includes data from ~25 sequentially recorded ion mobility distributions. A summary of threshold transition times and rates of conversions between different structures for these states is provided in Table 1.

It is instructive to consider the changes in populations that are observed for the +7 and +8 charge states in detail. Because it is relatively simple, we begin this discussion by considering the +8 charge state. Figure 5 shows that after an initial induction period the peak associated with partially folded B and C ions rapidly disappears. At the same time, peaks associated with the D and E states are observed. For trapping times in excess of ~40 ms, the abundance of D and E states is relatively constant, with populations of ~10% and 90%, respectively. The D and E states must interconvert on time scales that are much longer than those that we have investigated.

Some insight about the time scales required for states D and E to interconvert may come from the FTMS isotopic exchange studies. Using similar ESI conditions, Freitas et al.[12] measured two populations of +8 ions after exposure to 2×10^{-7} Torr of

TABLE 1: Measured Transition Times for Ubiquitin Ions Stored in an Ion Trap at 300 K

charge state	transition type	threshold time (ms)[a]	time required to reach midpoint (ms)[b]	rate of depletion of compact ions (s^{-1})[c]
+6	depletion of A	100	500	0.2
+7	depletion of A	30	37	49
	depletion of A′	575	400	0.3
	depletion of A″	1750	6310	0.005
	formation of B/C/D	35	37	
	formation of B/C/D′	1750	6400	
	formation of E	35	40	
	formation of E′	500	320	
+8	depletion of B/C	25	35	240
	formation of D	35	37.5	
	formation of E	27.5	35	

[a] Time at which compact ion begins to unfold. Calculated by examining the first derivative of the plot of relative ion intensity versus time. [b] Time at which the relative ion intensity reaches 50% of the difference between the initial and final intensities. [c] Rates were obtained from the slope of the plot of the natural logarithm of the compact ion relative intensity versus time over the region where the compact ion unfolds.

D_2O for 1.0 h: a state that comprises ~92% of the distribution and incorporates ~85 deuteriums and a state that comprises ~8% of the population and incorporates only ~72 deuteriums. As shown in Figure 5, these populations are similar to those that we have recorded at our longest times for states D and E. Additionally, one might expect a restricted exchange level on a relatively compact state (D), since some folding may protect some internal sites. We have previously shown that this is the case for compact and elongated states of cytochrome *c* ions when exchange is carried out at 300 K.[21] Inclusion of the populations at 3600 s in Figure 5 suggests that the populations of D and E states of the +8 charge state are formed early in the electrospray process, but they appear to remain stable over remarkably extended periods.

The +7 charge state shows substantially more complicated behavior. Figure 6 shows that compact states dominate the distribution at short trapping times (<35 ms); however, after this time, the fraction of the compact states rapidly decreases (to ~35% of the total ion population) and two new peaks, corresponding to partially folded B/C/D states, and the elongated E conformers are observed. The observation that ~65% of the compact state population unfolds rapidly, while ~35% persists to longer times, indicates that there are at least two populations of compact states.

(Below, we provide evidence for three states. We note that while the multiplicity of states having identical cross sections is clear from plots of the time-profiles for those states that decay, when new states, produced at different times, have identical cross sections an ambiguity about whether they are distinct arises. That is, it is possible that identical states are formed through different unfolding pathways. For this discussion, we include the possibility that new states having identical cross sections may be different structures by also denoting these states with primes.)

The loss of population associated with state A and onsets of peaks corresponding to B/C/D and E states occurs at 35 ± 5 ms, identical within our time resolution. However, the intensity of the B/C/D peak increases more rapidly than does the intensity for the peak for the E state. At 100 ms, the B/C/D states comprise ~48% of the population: about three times the ~15% population of the E state. We speculate that this may indicate that the fraction of the compact state that rapidly unfolds (state A) does so in a statistical fashion. That is, there are four general pathways for unfolding that have similar accessibilities after ~35 ms.

At longer trapping times, the changes in population of the compact state relative to others that are formed suggest that there are two additional compact states. From ~250 ms to 1.0 s, some of the remaining population of the compact state (referred to as A′) appears to unfold directly to the elongated state. Although it is possible that the elongated state formed from A′ is the same as that formed from A, this need not be the case; therefore, we distinguish this transition by denoting the increase in the population of elongated states between ~250 ms and 1.0 s as a new state E′. While the fraction of the E′ state increases from ~18 to 30% over the ~250 ms to 1.0 s time period, the abundance of compact ions decreases from ~30 to 25%. Additionally, the increase in the population of elongated states appears to be associated with the B/C/D conformers. From ~250 ms to 1.0 s, the abundances of peaks associated with the B/C/D conformers decrease slightly, from ~50% to ~45% for states B/C/D. The combined decrease of peaks associated with the A′ and B/C/D states (from ~250 ms to 1.0 s) appears to explain the corresponding increase in elongated E′ ions.

At even longer times (>1 s) an additional process, which appears to be associated with an increase in the population of partially folded ions, depletes much of the remaining fraction of compact states. This process appears to be substantially slower than the A′ → E′ transition. Thus, there is evidence for a third compact state, A″, which is very stable and survives to long times. The A″ state eventually unfolds to partially folded states; however, unlike the other compact A or A′ states, it does not appear to form elongated E states. The partially folded states that are formed from unfolding of A″ may have different structures than the B/C/D forms that arose directly from A. Therefore, we define them as new partially folded states B/C/D′.

Our longest trapping time experiments 30 s give populations of ~65, 28, and 7% for the partially folded (B/C/D′), elongated E′, and remaining compact states, respectively. It is interesting to compare these results to the populations and peak shapes observed in FTMS isotopic exchange studies of the +7 charge state. After a 1.0 h exposure to 2×10^{-7} Torr of D_2O the +7 state shows evidence for three different conformations. The most abundant state (~60%of the population) incorporates 89 deuteriums, and the well-resolved peak shape is analogous to the +8 charge state feature that we assigned to the E′ state. Based on the similarities associated with deuterium incorporation for the +8 charge state (and also +9), we speculate that this feature corresponds to elongated E′ state ions in the +7 charge state. The remaining population is distributed over a broad feature that appears to correspond to two states. One state (~30% of the population) incorporates ~70 deuteriums; the remaining ~10% of the population incorporates fewer deuteriums, ~60. Based on similarities with the +8 state, and also the trends observed at our longest trapping times, we speculate that the state which incorporates 60 deuteriums may be due to a small remaining population of compact conformers (A″); additionally, the state with an incorporation level of 70 deuteriums might correspond to a partially folded state. These assignments suggest that the B/C/D′ states continue to unfold at times in excess of 30 s such that eventually the population of elongated conformers dominates the distribution.

Finally, it is worthwhile to note that we do not fully understand the initial induction periods associated with early structural transitions in these data. We have previously suggested

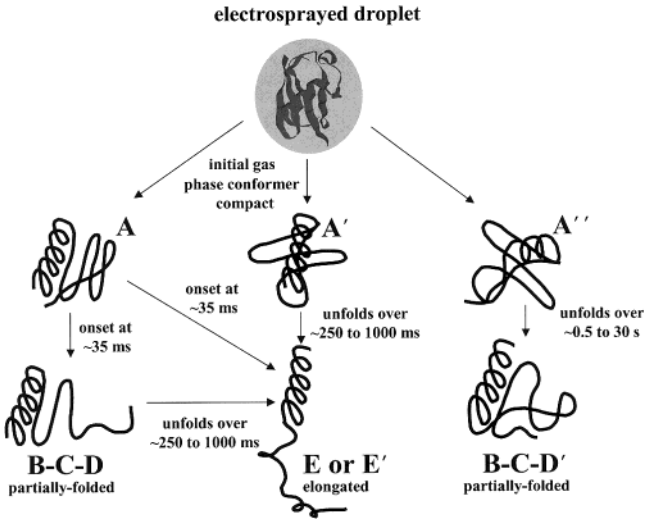

Figure 7. Schematic illustration of structural transitions that are observed upon electrospray ionization of ubiquitin to produce the +7 charge state.

that solvent evaporation during the ESI process should cool the internal temperatures of these ions. If this cooling process were to cool internal modes below the ambient temperature of the trap, then the induction period might be associated with the time required for ions to warm. We are currently considering several other explanations and will discuss this phenomenon further in the future.

Pathways for Forming Gas-Phase Conformations for the +7 Charge State. It is useful to summarize the transitions that were observed for the +7 charge state with the simple scheme in Figure 7. The +7 charge state initiates from the electrosprayed droplet in three types of distinguishable compact states A, A′, and A″. After a short delay, the A state abruptly unfolds to the partially folded B/C/D and elongated E states. At longer times, some of the B/C/D ions appear to continue to unfold, producing elongated E ions. An additional population of compact conformers A′ appears to be substantially more stable than the A form. The A″ state forms a partially unfolded state that persists to long times. These partially unfolded ions are referred to as B/C/D′. Unlike the B/C/D state, they do not appear to unfold to the E state (over the time scale of our experiments).

Summary and Conclusions

The conformations of the +6, +7, and +8 charge states of electrosprayed ubiquitin ions have been examined using an ion trapping/ion mobility/mass spectrometry approach. In this approach, ions are stored in an ion trap for variable time periods ranging from ~10 ms to 30 s, during which time structural changes may occur. By varying the trapping delay times in small increments (<ms increments are possible) it is possible to accumulate a profile of how the populations of different states change in time. The approach has merit as a simple method of obtaining kinetic information (e.g., the data in Table 1) and pathways for structural changes. Kinetic information has been obtained previously from mobility experiments by varying the time that ions spend drifting across the drift tube (controlled by varying the drift field). In practice it is only about an order of magnitude time variation that is possible by varying the drift field, and data analysis is complicated because the positions and shapes of peaks in the drift time distributions, as well as the instrumental resolving power, vary with the drift field.

The present results for ubiquitin provide a detailed look at how the ions change as they emerge from the electrospray droplet into the gas phase. It appears that the +6 to +8 states initiate as relatively compact conformations. The time required for structural transitions depends on the charge state, as well as the initial conformation. The +6 charge state initiates primarily as a compact state, and only small changes in the population of this state are observed, even at our longest trapping times. The +8 state initiates as partially folded states. After an initial induction period, these states rapidly unfold to more elongated structures that do not appear to interconvert. Substantially more complex behavior is observed for the +7 charge state. There is evidence that protein ions in the +7 charge state exist initially in several different compact states, and a scheme involving multiple pathways is proposed to explain the experimental results. In the end, there are several pathways associated with the unfolding transitions that are observed. From the present results, we still cannot discern whether structures formed from different pathways (having the same collision cross sections) are distinct; however, it is clear that for the +7 state there are many more transitions between compact, partially folded and elongated states than were proposed previously from studies as a function of injection energy or source temperature.[7,8]

Finally, the ability to record mobility distributions for ions that have been trapped for variable times, allows comparisons of mobility results with other measurements to be made. Some additional progress in correlating cross section data with isotopic exchange studies by FTMS have been made for the +6 to +8 ions of ubiquitin. For example, the relatively long lifetime of the compact +6 charge state is consistent with the wide isotopic exchange recorded by FTMS. For +8 ions, the population recorded at our longest time for states D and E appears to be similar to states that incorporate ~72 and 85 deuteriums, respectively. The conformers observed for the +7 charge states have been correlated to FTMS exchange level data. Efforts to make additional comparisons of mobility experiments with other techniques for other systems are underway in our laboratory.

Acknowledgment. This work is supported in part by the National Science Foundation (Grant No. CHE-0078737). E.R.B. was supported by a grant to the Indiana Instrumentation Institute from the Indiana 21st Century fund. The authors also acknowledge many helpful comments from their co-workers, Stephen J. Valentine, Anne E. Counterman, and Cherokee S. Hoaglund-Hyzer, and also thank Fred McLafferty for providing preprints of unpublished work.

References and Notes

(1) For a discussion, see for example: Kim, P. S.; Baldwin, R. L. *Annu. Rev. Biochem.* **1990**, *49*, 631. Lumry, R.; Eyring, H. *J. Phys. Chem.* **1954**, *58*, 110. Creighton, T. E. *Prog. Biophys. Mol. Biol.* **1978**, *33*, 231. Roder, H.; Elove, G. A.; Englander, S. W. *Nature*, **1988**, *335*, 700. Englander, S. W. *Science*, **1993**, *262*, 848. Richards, F. M. *Sci. Am.* **1991**, *Jan*, 54.

(2) Fenn, J. B.; Mann, M.; Meng, C. K.; Wong, S. F.; Whitehouse, C. M. *Science* **1989**, *246*, 614.

(3) Several recent reviews of this type of work include: Williams, E. R. *J. Mass. Spectrom.* **1996**, *31*, 831. Green, M. K.; Lebrialla, C. B. *Mass Spectrom. Rev.* **1997**, *16*, 53. Clemmer, D. E.; Jarrold, M. F. *J. Mass Spectrom.* **1997**, *32*, 577. Hoaglund-Hyzer, C. S.; Counterman, A. E.; Clemmer, D. E. *Chem. Rev.* **1999**, *99*, 3037.

(4) Lau, Y. K.; Ikuta, S.; Kebarle, P. *J. Am. Chem. Soc.* **1982**, *104*, 1462. Klassen, J. S.; Blades, A. T.; Kebarle, P. *J. Phys. Chem.* **1995**, *99*, 15509. Woenckhaus, J.; Hudgins, R. R.; Jarrold, M. F.; *J. Am. Chem. Soc.* **1997**, *119*, 9586. Fye, J. L.; Woenckhaus, J.; Jarrold, M. F. *J. Am. Chem. Soc.* **1998**, *120*, 1327.

(5) Rodriguez-Cruz, S. E.; Klassen, J. S.; Williams, E. R. *J. Am. Soc. Mass Spectrom.* **1997**, *8*, 565.

(6) Lee, S.-W.; Freivogel, P.; Schindler, T.; Beauchamp, J. L. *J. Am. Chem. Soc.* **1998**, *120*, 11758.

(7) Valentine, S. J.; Counterman, A. E.; Clemmer, D. E. *J. Am. Soc. Mass Spectrom.* **1997**, *8*, 954.

(8) Li, J.; Taraszka, J. A.; Counterman, A. E.; Clemmer, D. E. *Int. J. Mass Spectrom.* **1999**, *185/186/187*, 37.

(9) Covey, T.; Douglas, D. J. *J. Am. Soc. Mass Spectrom.* **1993**, *4*, 616.

(10) Zhang, X.; Cassady, C. J. *J. Am. Soc. Mass Spectrom.* **1996**, *7*, 1211.

(11) Wyttenbach, T.; Kemper, P. R.; Bowers, M. T. *Int. J. Mass Spectrom.* **2002**, *212*, 13.

(12) Freitas, M.; Marshall, A. G. *Int. J. Mass Spectrom.* **1999**, *185/186/187*, 565.

(13) Breuker, K.; Oh, H.; Horn, D. M.; Cerda, B. A.; McLafferty, F. W. *J. Am. Chem. Soc.* **2002**, *124*(22), 6407.

(14) Purves, R. W.; Barnett, D. A.; Ells, B.; Guevremont, R. *J. Am. Soc. Mass Spectrom.* **2000**, *11*, 738. Purves, R. W.; Barnett, D. A.; Ells, B.; Guevremont, R. *J. Am. Soc. Mass Spectrom.* **2001**, *12*, 894.

(15) Badman, E. R.; Hoaglund-Hyzer, C. S.; Clemmer, D. E. *Anal. Chem.* **2001**, *73*, 6000.

(16) Hagen, D. F. *Anal. Chem.* **1979**, *51*, 870. Hill, H. H.; Siems, W. F.; St. Louis, R. H.; McMinn, D. G. *Anal. Chem.* **1990**, *62*, 1201A.

(17) Clemmer, D. E.; Jarrold, M. F. *J. Mass Spectrom.* **1997**, *32*, 577.

(18) Mason, E. A.; McDaniel, E. W. *Transport Properties of Ions in Gases*; Wiley: New York, 1988.

(19) As noted previously, to determine t_D it is necessary to correct the raw arrival time measurements by the time that the ions spend traveling through other portions of the instrument. This correction is normally small ($\sim$80 to 150 μs) relative to the time spent in the drift tube.

(20) Goeringer D. E.; Asano, K. G.; McLuckey, S. A. *Int. J. Mass Spectrom. 182/183*, **1999**, 275.

(21) Valentine, S. J.; Clemmer, D. E. *J. Am. Chem. Soc.*, **1997**, *119*, 3558.